BIOLOGY OF REPRODUCTION **72,** 328–337 (2005)
Published online before print 29 September 2004.
DOI 10.1095/biolreprod.104.034470

Localization and Significance of Molecular Chaperones, Heat Shock Protein 1, and Tumor Rejection Antigen gp96 in the Male Reproductive Tract and During Capacitation and Acrosome Reaction[1]

Kelly L. Asquith,[3] Amanda J. Harman,[3] Eileen A. McLaughlin,[3,4] Brett Nixon,[3] and R. John Aitken[2,3,4]

Reproductive Science Group,[3] School of Environmental and Life Sciences, University of Newcastle, Callaghan, New South Wales 2308, Australia
ARC Centre of Excellence in Biotechnology and Development,[4] School of Environmental and Life Sciences, University of Newcastle, Callaghan, New South Wales 2308, Australia

ABSTRACT

Although the molecular basis of sperm-oocyte interaction is unclear, recent studies have implicated two chaperone proteins, heat shock protein 1 (HSPD1; previously known as heat shock protein 60) and tumor rejection antigen gp96 (TRA1; previously known as endoplasmin), in the formation of a functional zona-receptor complex on the surface of mammalian spermatozoa. The current study was undertaken to investigate the expression of these chaperones during the ontogeny of male germ cells through spermatogenesis, epididymal sperm maturation, capacitation, and acrosomal exocytosis. In testicular sections, both HSPD1 and TRA1 were closely associated with the mitochondria of spermatogonia and primary spermatocytes. However, this labeling pattern disappeared from the male germ line during spermiogenesis to become undetectable in testicular spermatozoa. Subsequently, these chaperones could be detected in epididymal spermatozoa and in previously unreported "dense bodies" in the epididymal lumen. The latter appeared in the precise region of the epididymis (proximal corpus), where spermatozoa acquire the capacity to recognize and bind to the zona pellucida, implicating these structures in the functional remodeling of the sperm surface during epididymal maturation. Both HSPD1 and TRA1 were subsequently found to become coexpressed on the surface of live mouse spermatozoa following capacitation in vitro and were lost once these cells had undergone the acrosome reaction, as would be expected of cell surface molecules involved in sperm-egg interaction. These data reinforce the notion that these chaperones are intimately involved in the mechanisms by which mammalian spermatozoa both acquire and express their ability to recognize the zona pellucida.

acrosome reaction, chaperone, epididymis, fertilization, gamete biology, signal transduction, testis

INTRODUCTION

Following spermatogenesis, spermatozoa leave the testis in a structurally complete but functionally deficient form, incapable of progressive motility, oocyte recognition, and acrosomal exocytosis. Functional competence is acquired during passage through the epididymal lumen. The biochemical basis of sperm maturation in the epididymis has been extensively studied, and it is now well established that the composition and localization of sperm membrane proteins changes significantly during this process (reviewed in [1]). However, the precise mechanism by which spermatozoa acquire the potential for sperm-zona interaction during epididymal transit has yet to be elucidated.

Gamete interaction in mammals comprises a complex series of cellular interactions culminating in fertilization of the oocyte by a single spermatozoon. This process begins in the female reproductive tract, where spermatozoa undergo a postejaculatory maturation process termed capacitation, which results in these cells gaining the competence to recognize and bind to the extracellular matrix surrounding the oocyte, the zona pellucida [2, 3]. Although much is known about the importance of ZP3 as the zona glycoprotein primarily responsible for sperm binding during the initial stages of fertilization, little is known about the corresponding zona receptor on the sperm surface. A number of candidate molecules has been proposed, including galactosyltransferase, sp56, zonadhesin, and zona receptor kinase (reviewed in [4, 5]). It has been speculated that the diverse nature of these proposed zona receptor molecules can be attributed to interspecies variation in the biochemical mechanisms that regulate sperm-zona interaction. It is also possible that this process involves the coordinated action of several sperm proteins, each with a specific role at different stages of the recognition process [6, 7]. Experimental limitations are also imposed by sperm populations being heterogeneous; a typical sperm preparation contains cells at various stages of maturity, only a minority of which have attained a state of capacitation that is compatible with zona binding [8].

Phosphorylation of sperm proteins on tyrosine residues has been shown to be an important correlate of capacitation in all mammalian species studied to date [9–13]. A recent study from our laboratory demonstrated a causal relationship between this phosphorylation event and the ability to bind the zona pellucida [8]. Furthermore, we established that tyrosine phosphoproteins localized on the sperm surface overlying the acrosome have a critical role in sperm-zona interaction. Proteomic analysis revealed that two of the major proteins that are tyrosine phosphorylated and localized to the surface of murine spermatozoa during capacitation are the molecular chaperones, heat shock protein 1 (HSPD1; previously known as heat shock protein 60 [HSP60]) and tumor rejection antigen 1 (TRA1; previously known as endoplasmin [ERP99], a member of the heat

[1]This work was supported by Schering AG and the NHMRC.
[2]Correspondence: R. John Aitken, ARC Centre of Excellence in Biotechnology and Development, School of Environmental and Life Sciences, University of Newcastle, Callaghan, NSW 2308, Australia.
FAX: 61 2 49 21 6308; e-mail: jaitken@mail.newcastle.edu.au

Received: 19 July 2004.
First decision: 7 August 2004.
Accepted: 16 September 2004.

ISSN: 0006-3363. http://www.biolreprod.org

shock protein 90 family). We have hypothesized that these proteins may form part of a multimeric zona pellucida receptor complex that is assembled on the surface of murine spermatozoa during capacitation [8].

Examination of the expression patterns for HSPD1 and TRA1 during epididymal maturation, capacitation, and the acrosome reaction is a necessity if we are to understand the function of these proteins during fertilization. HSPD1 has previously been reported in the testes of rats, humans, and monkeys [14–16]. However, no previous studies have been performed on the expression of HSPD1 on testicular germ cells in the mouse or, indeed, during posttesticular epididymal sperm maturation for any mammalian species. Similarly, the distribution of TRA1 has not previously been reported during the differentiation and maturation of male gametes. The purpose of the current study was to address these deficiencies in our knowledge and further elucidate the roles of HSPD1 and TRA1 in the differentiation of functional spermatozoa.

MATERIALS AND METHODS

Antibodies

Antichaperone primary antibodies were obtained from Santa Cruz Biotechnology (Santa Cruz, CA). Two affinity-purified polyclonal antibodies against each protein were used for Western blotting and immunolocalization, designated HSPD1-1 (anti-HSP60 H-300; raised against an epitope corresponding to amino acids 274–573 at the carboxy terminus of heat shock protein 1), HSPD1-2 (anti-HSP60 N-20; raised against a peptide mapping to the amino terminus of heat shock protein 1), TRA1-1 (anti-GRP94 C-19; raised against a peptide mapping to the carboxy terminus of tumor rejection antigen gp96), and TRA1-2 (anti-GRP94 H-212; raised against a recombinant protein corresponding to amino acids 200–411 mapping near the carboxy terminus of tumor rejection antigen gp96). Anti-CD45 antibody was used as a negative control for live immunodetection assays (BD Transduction Laboratories, Lexington, KY). Sigma-Aldrich (Castle Hill, Australia) supplied the anti-α-tubulin (B-5-1-2), fluorescein isothionate (FITC)-conjugated, horseradish peroxidase (HRP)-conjugated and 10-nm gold-conjugate goat anti-rabbit and rabbit anti-goat immunoglobulins.

Other Reagents

Hepes, penicillin, and streptomycin were obtained from Gibco (Paisley, U.K.). BSA was obtained from Research Organics (Cleveland, OH). Minicomplete protease inhibitor tablets were from Roche (Mannheim, Germany). Nitrocellulose and Percoll were from Amersham (Buckinghamshire, U.K.). Mowiol 4-88 was from Calbiochem (La Jolla, CA). Paraformaldehyde, glutaraldehyde, LR white, nickel grids, and uranyl acetate were supplied by ProSciTech (Thuringowa, Australia). Protein G-coated Dynabeads were from Dynal (Oslo, Norway). Other reagents were from Sigma-Aldrich, unless otherwise stated.

Preparation of Epididymal Spermatozoa and Testicular Cells

All animal use was approved by the University of Newcastle Animal Ethics Committee and conducted in accordance with the International Guiding Principles for Biomedical Research Involving Animals. Spermatozoa were obtained from adult Swiss mice (age >8 wk; University of Newcastle Animal Facility) and maintained in Hepes-buffered Biggers Whitten Whittingham (BWW; [17]) media composed of 91.5 mM NaCl, 4.6 mM KCl, 1.7 mM $CaCl_2$, 1.2 mM KH_2PO_4, 1.2 mM $MgSO_4$, 25 mM $NaHCO_3$, 5.6 mM D-glucose, 0.27 mM sodium pyruvate, 44 mM sodium lactate, 5 U/ml penicillin, 5 μg/ml streptomycin, 20 mM Hepes buffer, and 0.3% w/v BSA. Caput epididymidal sperm were prepared by depositing the caput in BWW and piercing several times with a 25-gauge needle, after which gentle pressure was applied to release spermatozoa into the medium. These preparations contained some epithelial and blood cell contamination, and were therefore further purified by centrifugation through 30% v/v Percoll in PBS (pH 7.4) at 500 × *g* and 37°C for 15 min. The resultant pellet contained approximately 90% viable caput sperm as determined by propidium iodide staining. To prepare cauda epididymidal sperm, the cauda was deposited in BWW, a single tubule was cut, and gentle pressure was applied to release sperm into the medium. This preparation contained caudal sperm, free of any detectable cellular contamination. For capacitation, cauda sperm were diluted to 6×10^6 sperm/ml in BWW and incubated for 90 min at 37°C under an atmosphere of 5% CO_2:95% air. Following incubation, sperm were collected by centrifugation (500 × *g* for 3 min) and washed three times in PBS.

Total testicular cell preparations were obtained by macerating the testis tissue in BWW. Cells were then washed three times in PBS before protein extraction. These preparations contained both somatic and germ cells from the testis.

SDS-PAGE and Western Blotting

Proteins were extracted in a modified SDS-PAGE sample buffer (2% w/v SDS, 10% w/v sucrose in 0.1875 M Tris, pH 6.8) with protease inhibitor tablets, by incubation at 100°C for 5 min. Insoluble matter was removed by centrifugation at 20 000 × *g* for 10 min, and protein estimations were performed using the DC Protein Assay Kit (Bio-Rad, Hercules, CA).

Proteins were boiled in SDS-PAGE sample buffer (2% v/v mercaptoethanol, 2% w/v SDS, and 10% w/v sucrose in 0.1875 M Tris, pH 6.8, with bromophenol blue) and resolved by SDS-PAGE on polyacrylamide gels [18] followed by transfer onto nitrocellulose membranes [19]. Membranes were blocked with 3% w/v BSA in Tris-buffered saline (TBS; pH 7.4) for 1 h before being probed with 1:1000 dilutions of primary antibody in TBS containing 1% w/v BSA and 0.1% v/v polyoxyethylenesorbitan monolaurate (Tween-20; TBS-T) for 2 h at room temperature. Blots were washed three times in TBS-T followed by incubation with 1:1000 HRP-conjugated secondary antibody in 1% w/v BSA/TBS-T for 1 h. Following three washes in TBS-T, proteins were detected using an enhanced chemiluminescence kit (Amersham, Buckinghamshire, U.K.). Western blots were stripped in 100 mM mercaptoethanol, 2% w/v SDS, and 62.5 mM Tris (pH 6.7) at 60°C for 1 h, followed by several washes in TBS-T before reprobing.

Tissue Immunofluorescence

Tissue was collected from mouse testes and epididymides, fixed in formalin, embedded in paraffin, and cut into 5-μm sections. Following dewaxing and rehydration, antigen retrieval was performed by subjecting the slides to microwaves (500 W) for 20 min in citrate buffer (10 mM trisodium citrate, 4.4 mM HCl, pH 6.0). All subsequent incubations were performed at 37°C in a humid chamber, and all antibody dilutions and washes were conducted in PBS. Sections were blocked at 37°C for 1 h in 10% v/v serum supplemented with 3% w/v BSA in PBS. Slides were rinsed and incubated at 4°C overnight in 1:50 primary antibody. Following three washes, 1:100 dilutions of the corresponding FITC-conjugated secondary antibody were applied. Sections were washed three times and counterstained with 2 μg/ml propidium iodide, a nuclear dye included to aid visualization of the tissue structure. Slides were mounted in antifade medium (10% w/v mowiol 4-88 with 30% v/v glycerol in 0.2 M Tris [pH 8.5] with 2.5% w/v 1,4-diazobicyclo-[2.2.2]-octane) and viewed using an LSM510 laser scanning confocal microscope equipped with argon and helium/neon lasers (Carl Zeiss PTY, Sydney, Australia). Excitation wavelengths 48/545 and emission spectra 500–530 and >560 nm for FITC conjugates and propidium iodide, respectively.

Electron Microscopy

Mouse epididymides were fixed in 4% w/v paraformaldehyde/0.5% v/v glutaraldehyde in 0.1 M phosphate buffer (pH 7.3) followed by dehydration, infiltration, and embedding in LR White resin. Sections (70 nm) were cut on an Ultracut S ultramicrotome (Reichert-Jung, Austria) with a diamond knife (Diatome Ltd, Bienne, Switzerland) and placed on nickel grids. All antibody dilutions and washes for immunogold labeling were performed in Dulbecco PBS (DPBS; pH 7.4). Grids were treated with 0.05 M glycine dissolved in DPBS for 40 min followed by washing and blocking in 3% w/v BSA in DPBS for 1 h at 37°C. Primary antibody diluted to 1:25 was applied and incubated overnight at 4°C. Grids were washed and incubated with 1:20 dilutions of secondary antibody conjugated to 10-nm gold particles for 2 h at 37°C. After washing, sections were postfixed in 2% v/v glutaraldehyde, dried, and stained with 1% w/v uranyl acetate in 40% v/v methanol. Micrographs were taken on a JEOL-100CX transmission electron microscope (JEOL, Tokyo, Japan) operating at 80 kV.

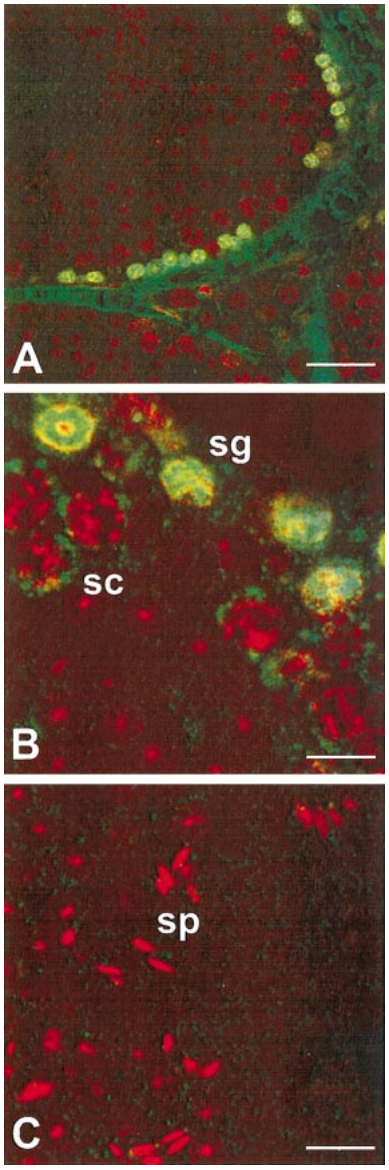

FIG. 1. Immunofluorescence of HSPD1-1 in the mouse testis. Testis sections were stained with anti-HSPD1-1 followed by FITC-conjugated secondary antibody (green) and counterstained with propidium iodide (red). HSPD1-1 labeling appeared in spermatogonia (sg) and spermatocytes (sc), but not in spermatozoa (sp). **A**) Bar = 40 μm. **B**) Bar = 10 μm. **C**) Bar = 15 μm.

Immunolocalization of Chaperones on Fixed Spermatozoa

Following incubation, spermatozoa were fixed in 1% w/v paraformaldehyde, washed three times with PBS, plated onto glass slides coated with 0.1% v/v poly-L-lysine, and air-dried. All subsequent incubations were performed at 37°C in a humid chamber, and all dilutions and washes were performed in PBS. Spermatozoa were permeabilized with 0.2% v/v Triton X-100 for 15 min, rinsed, and blocked in 10% v/v serum in 3% w/v BSA at 37°C for 1 h. Slides were rinsed and incubated at 4°C overnight in a 1:50 dilution of primary antibody. After three washes, cells were incubated with 1:100 FITC-conjugated secondary antibody at 37°C for 2 h, washed again, and mounted in antifade medium. Images were captured using a confocal microscope as described.

Immunodetection of Chaperones on Live Spermatozoa

Attempts to localize proteins on live mouse spermatozoa by immunofluorescence were hampered by the fragility of spermatozoa from this species. For this reason, a protocol was developed to assay live spermatozoa in a single step. Magnetic beads coated with protein G (Dynabeads) were washed three times in 0.1% w/v BSA in PBS followed by conjugation with primary antibody for 2 h at room temperature. Beads were washed three times with BWW and added to spermatozoa following 1 h of preincubation. The sperm/bead suspension was maintained at 37°C for a further 45 min with regular mixing. Wet mounts of the suspension were prepared and counterstained with 2 μg/ml propidium iodide for cell viability assessment. The percentage of viable sperm with bound antichaperone-coated beads was assessed by phase contrast and fluorescence microscopy with a Zeiss Axioplan 2 microscope (Carl Zeiss PTY). Negative controls consisted of beads that were either uncoated or coated with an antibody that does not bind to live sperm, anti-CD45.

Acrosome Reaction

Caudal epididymidal spermatozoa were capacitated as described above followed by 15 min of incubation in 1.25 μM calcium ionophore A23187. Vehicle (dimethyl sulfoxide) controls were included. Samples were then diluted 1:10 in prewarmed hyperosmotic swelling medium (25 mM sodium citrate, 75 mM fructose) and incubated at 37°C for 1 h. Spermatozoa were fixed in ice-cold 100% v/v methanol and air-dried onto poly-L-lysine coated slides. Following staining using the immunofluorescence protocol described above, cells were colabeled with tetramethylrhodamine isothiocyanate (TRITC)-conjugated *Arachis hypogaea* lectin (0.5 mg/ml in PBS) at room temperature for 20 min, washed, and mounted in antifade medium as above. Cells were scored on the basis of their viability, acrosomal status, and chaperone staining pattern.

Statistics

Experiments were replicated with material collected from at least three different animals, and the graphical data presented represent means ± SEM. Percentage data were subjected to arcsine transformation before performing an analysis of variance. Statistically significant differences between group means were tested using the Fisher protected least significant difference test. Samples with a P value < 0.05 were considered significant.

RESULTS

HSPD1 and TRA1 Are Localized on Precursor Germ Cells but Not on Spermatozoa in the Testes

Laser scanning confocal microscopy and indirect immunofluorescence were used to reveal chaperone localization, and all sections were counterstained with a nuclear dye, propidium iodide, to facilitate visualization of the tubule structure and assist in identifying labeled cell types. Anti-HSPD1-1 labeling in the testis was restricted to spermatogonia and spermatocytes, with no staining apparent on mature spermatozoa (Fig. 1). The staining was particularly dense in the spermatogonia and was confined to subcellular structures distributed throughout the cytoplasm, which is consistent with germ cell mitochondria. In primary spermatocytes, the punctate staining pattern was significantly reduced and, by the spermatid stage, no labeling was evident. Furthermore, no signals could be detected emanating from the spermatozoa present in the lumina of the seminiferous tubules. It is intriguing that the anti-HSPD1-2 antibody failed to generate any positive signals in testicular tissues by immunocytochemistry, despite its positive activity by Western blot analysis (see Fig. 3B). Presumably, the epitopes recognized by this antibody were not exposed in the testicular germ cell population, despite the rigorous antigen retrieval protocols applied in this analysis.

The localization of tumor rejection antigen gp96 in the testis was examined using the two polyclonal antibodies, anti-TRA1-1 and anti-TRA1-2. Both antibodies labeled discrete subcellular structures, putatively belonging to the endoplasmic reticulum, in spermatogonia, spermatocytes, spermatids, and residual bodies in mouse testis sections (Fig. 2). Again, no staining was apparent on spermatozoa present in the lumina of the seminiferous tubules (Fig. 2).

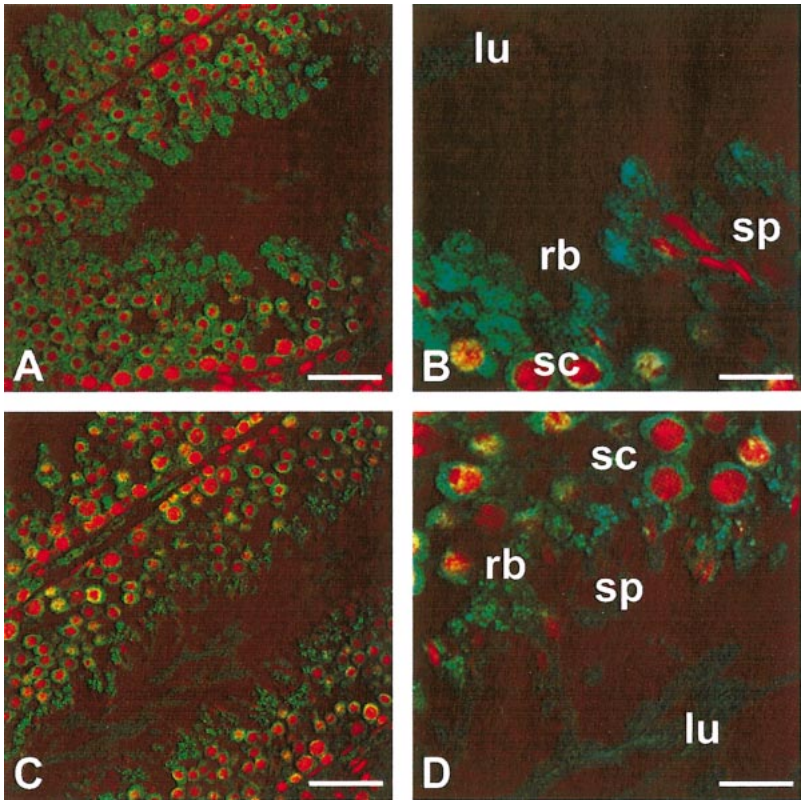

FIG. 2. Immunofluorescence of TRA1 in the mouse testis. Testis sections were stained with anti-TRA1 followed by FITC-conjugated secondary antibody (green) and counterstained with propidium iodide (red). **A**) Anti-TRA1-1 (bar = 40 μm). **B**) Anti-TRA1-1 (bar = 15 μm). **C**) Anti-TRA1-2 (bar = 40 μm). **D**) Anti-TRA1-2 (bar = 15 μm). Both antibodies labeled spermatogonia, spermatocytes (sc), and residual bodies (rb) but not spermatozoa (sp) in the lumen (lu) of the epididymis.

HSPD1 and TRA1 Are Expressed in the Epididymis

Attempts to generate purified sperm populations from the testes for Western blot analysis were unsuccessful. However, these cells could be isolated with more than 98% purity from both the caput and cauda epididymidis. Western blot analyses revealed that both HSPD1 and TRA1 are expressed in caput, corpus, and cauda spermatozoa (Fig. 3A). Both proteins were detected with each of the polyclonal antibodies employed in this study. Importantly, only one protein product with the same molecular mass was detectable with each antibody. By reprobing the membranes with anti-α-tubulin antibody as a loading control, we were able to determine that the relative levels of these proteins did not change dramatically in the spermatozoa as these cells migrated from the caput to the cauda. Although purified spermatozoa could not be obtained from the testis, comparison of Western blots of total testicular cell preparations with purified cauda epididymal spermatozoa revealed no perceivable differences in molecular weight or expression levels of HSPD1 or TRA1 between these regions (Fig. 3B).

Chaperones Are Localized on the Sperm Head and on Dense Bodies in the Epididymal Lumen

Anti-HSPD1-1 labeled the epididymal epithelium and a region of the sperm head overlying the acrosome in all spermatozoa. This labeling pattern was consistent within caput, corpus, and cauda epididymidis sections (Fig. 4). In contrast, although anti-HSPD1-2 also labeled the epithelium, it did not label spermatozoa. Instead, this antibody exhibited discrete areas of labeling in the lumen in the corpus and cauda, but not caput epididymis (Fig. 4). These discrete areas of labeling, referred to as dense bodies, were further investigated by electron microscopy (see below).

Considerable differences were also found in the labeling patterns exhibited by the two TRA1 antibodies. Anti-TRA1-1 showed a similar pattern to that of anti-HSPD1-1, labeling the epididymal epithelium and a region of the sperm head overlying the acrosome in the caput, corpus, and cauda epididymis (Fig. 5). On the other hand, anti-TRA1-2 labeled the epithelium as well as the dense bodies labeled with the anti-HSPD1-2 antibody in the corpus and cauda epididymidis, but never the caput region (Fig. 5).

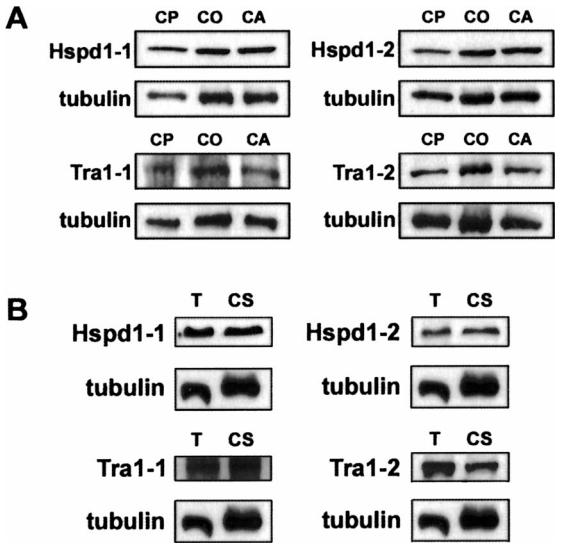

FIG. 3. Western blot analysis of HSPD1 and TRA1 in the mouse testis and epididymis. Cell extracts (5 μg) were resolved by SDS-PAGE and immunoblotted with anti-HSPD1-1, anti-HSPD1-2, anti-TRA1-1, and anti-TRA1-2. Each blot was reprobed with anti-α-tubulin to confirm equal protein loading in each lane. **A**) Purified sperm from mouse caput (CP), corpus (CO), and cauda (CA) epididymides. **B**) Mouse testis total cell extract (T) and purified cauda epididymidal sperm (CS).

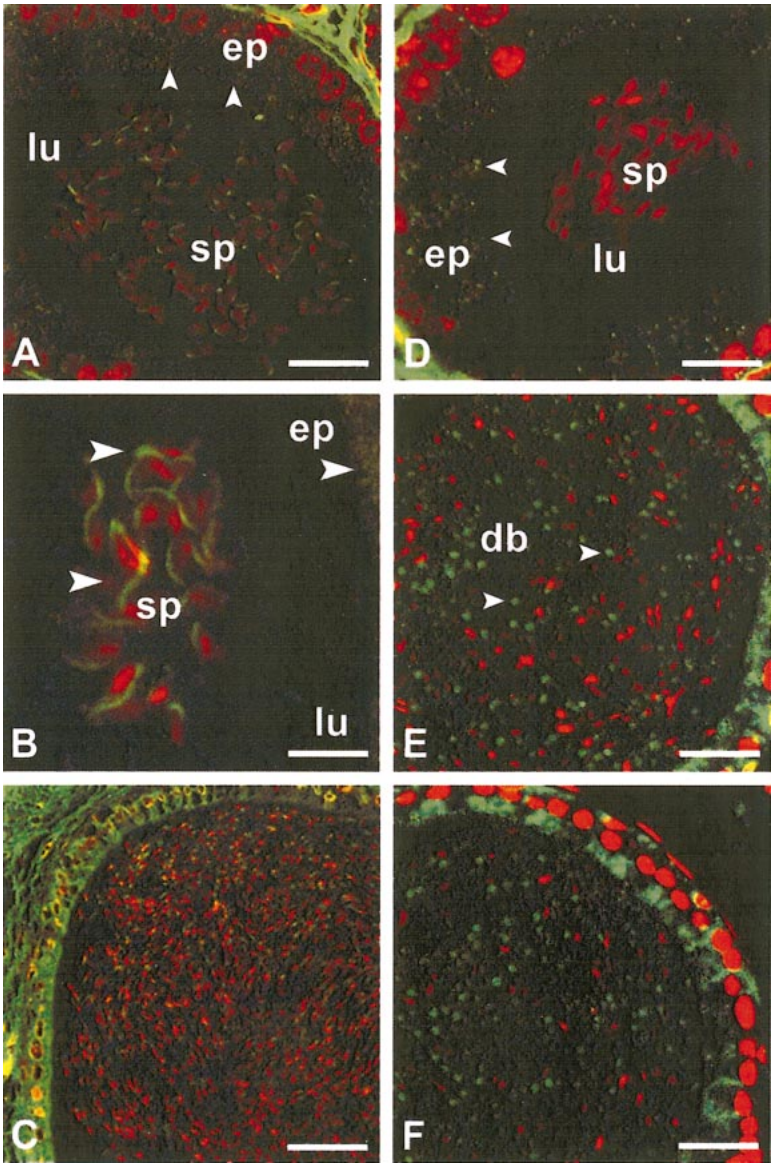

FIG. 4. Immunofluorescence of HSPD1 in the mouse epididymis. Epididymal sections were stained with anti-HSPD1 followed by FITC-conjugated secondary antibody (green) and counterstained with propidium iodide (red). Anti-HSPD1-1 labeling appeared in the epididymal epithelium (ep) and on the sperm (sp) head in the lumen (lu) of the epididymis. **A**) Caput (bar = 20 μm). **B**) Corpus (bar = 10 μm). **C**) Cauda (bar = 40 μm). Anti-HSPD1-2 also labeled the epithelium but did not label sperm. Discrete areas of labeling were evident within the lumen of the corpus and cauda but not caput epididymidis. These structures were termed dense bodies (db). **D**) Caput (bar = 10 μm). **E**) Corpus (bar = 20 μm). **F**) Cauda (bar = 23 μm).

Anti-TRA1-2 therefore gave an overall staining pattern that was identical to that observed with anti-HSPD1-2.

Immunogold Labeling of HSPD1 and TRA1 on Dense Bodies in the Epididymis

Ultrathin sections from the caput, corpus, and cauda mouse epididymides incubated with anti-HSPD1-2 and anti-TRA1-2 showed heavy labeling on dense structures residing in the epididymal lumen (Fig. 6). These structures ranged in diameter from 500 nm to 1.2 μm, with an average size of approximately 900 nm, and appeared as concentrated electron-dense regions with no apparent structural elements such as plasma membrane or organelles. Consistent with the immunofluorescence studies, these structures were observed in the corpus and cauda, but not the caput epididymis. These ''dense bodies'' were often present in close proximity to spermatozoa (Fig. 6B), although the HSPD1 and TRA1 epitopes expressed by the dense bodies were never observed on the spermatozoa themselves.

Chaperones Are Expressed on the Surface of Live Sperm in a Capacitation-Dependent Manner

Expression of HSPD1 and TRA1 over the acrosomal domain of epididymidal spermatozoa is suggestive of a function in gamete interaction. However, to be certain that these proteins are available on the surface of the sperm head for regulating interactions with the oocyte, antigen localization studies were performed on live cells. In uncapacitated sperm populations, anti-HSPD1-1 and anti-TRA1-1 labeled beads were observed binding to the surface of around 6% of cells, but on no other region of viable, motile spermatozoa (Fig. 7). Following capacitation, there was a dramatic increase ($P < 0.01$) in the proportion of spermatozoa expressing both anti-HSPD1-1 (27% ± 4%) and anti-ra1-1 (22% ± 5%) on the sperm head (Fig. 7). Labeling of capacitated spermatozoa with both antibodies was also significantly ($P < 0.001$) higher than when capacitated sperm were incubated with anti-CD45 or uncoated beads.

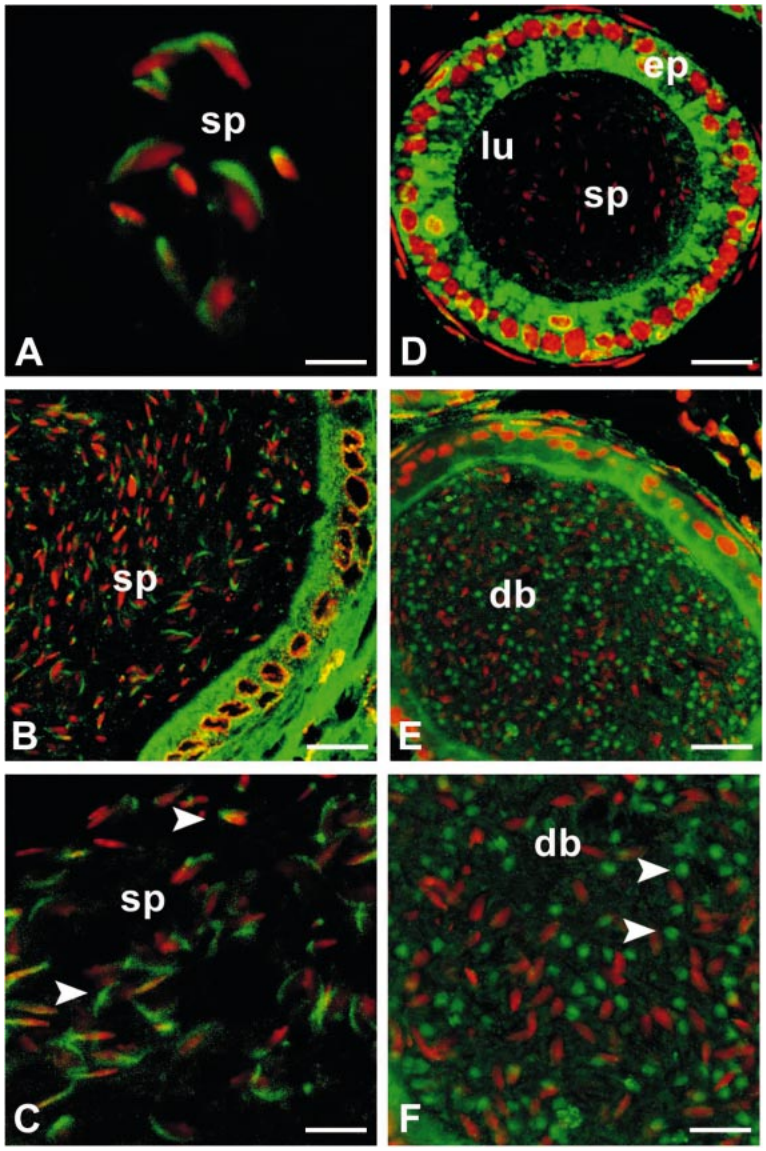

FIG. 5. Immunofluorescence of TRA1 in the mouse epididymis. Epididymal sections were stained with anti-TRA1 followed by FITC-conjugated secondary antibody (green) and counterstained with propidium iodide (red). Anti-TRA1-1 labeling appeared in the epididymal epithelium (ep) and on the sperm (sp) head in the lumen (lu) of the epididymis along the length of the duct. **A**) Caput (bar = 5 μm). **B**) Corpus (bar = 25 μm). **C**) Cauda (bar = 10 μm, arrows indicate sperm labeling). Anti-TRA1-2 also labeled the epithelium but did not label sperm. Discrete areas of labeling were evident within the lumen of the corpus and cauda but not caput epididymis. These structures were termed dense bodies (db). **D**) Caput (bar = 30 μm). **E**) Corpus (bar = 30 μm). **F**) Cauda (bar = 14 μm; arrows indicate db labeling).

Acrosomal Loss Is Correlated with Loss of Chaperones from the Sperm Head

Confirmation of the surface localization of the phosphorylated chaperones was achieved by following their fate subsequent to the induction of acrosomal exocytosis. For these studies, cauda epididymidal sperm were capacitated and the acrosome reaction was induced using the calcium ionophore A23187. Cells were stained with the antichaperone antibodies anti-HSPD1-1 and anti-TRA1-1, followed by FITC-conjugated secondary antibodies (green labeling in Fig. 8), and counterstained with TRITC-*Arachis hypogaea* lectin, which stains acrosome-intact but not acrosome-reacted cells (red labeling in Fig. 8). Overlay analysis revealed that all cells stained with either anti-HSPD1-1 (Fig. 8) or anti-TRA1-1 (data not shown) were acrosome intact, whereas all cells that had lost their acrosomes had also lost their chaperone labeling. A minimum of 200 cells were scored for each treatment.

DISCUSSION

A previous report from our laboratory described a causal relationship between expression of tyrosine phosphoproteins on the sperm surface following capacitation and the ability of these cells to bind to the zona pellucida. Mass spectrometry analysis identified HSPD1 and TRA1 as two of the key tyrosine-phosphorylated proteins involved in expression of this receptor activity [8]. In light of these data, the current study sought to enhance our understanding of the complex relationships between the development of mature functional spermatozoa capable of fertilization and the expression patterns for both HSPD1 and TRA1. For the first time, we describe the localization of these chaperones during spermatogenesis, epididymal maturation, and capacitation, and suggest important roles for HSPD1 and TRA1 in the mechanisms by which spermatozoa acquire and, ultimately, express their potential for sperm-zona interaction.

Labeling of testicular sections with anti-HSPD1-1 revealed a punctate localization pattern exclusively on spermatogonia and primary spermatocytes. No labeling was apparent on secondary spermatocytes, spermatids, or testicular spermatozoa. These data suggest a key role for HSPD1 during the mitotic stages of spermatogenesis and, because HSPD1 is known to associate with mitochondria, it is probable that this molecule is an integral part of the mitochondrial protein import machinery in early, mitotically active

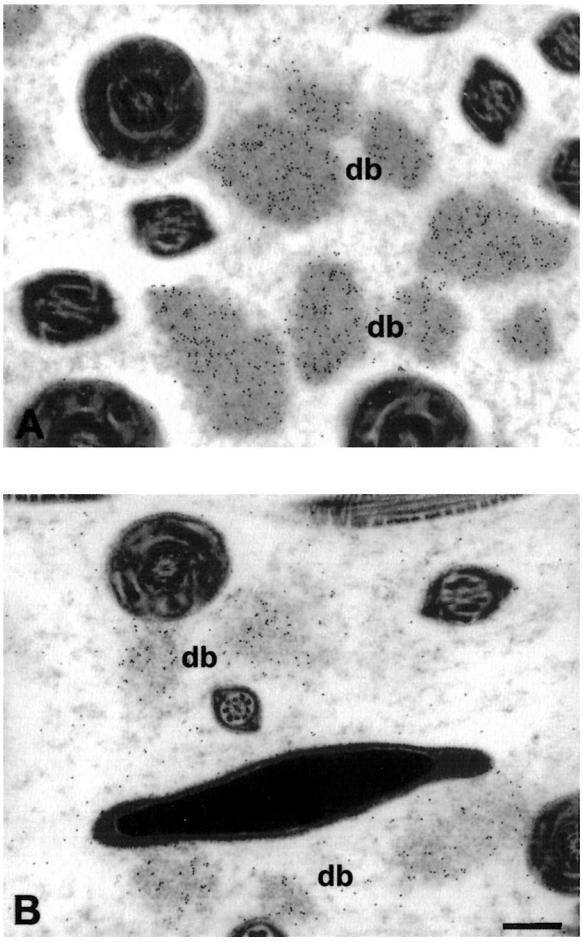

FIG. 6. Immunogold labeling of dense bodies within the mouse epididymis. Epididymal sections were stained with (**A**) anti-HSPD1-2 or (**B**) anti-TRA1-2 followed by secondary antibody conjugated to 10-nm gold. Heavily labeled dense bodies (db) were evident in the epididymal lumen. Bar represents 500 nm.

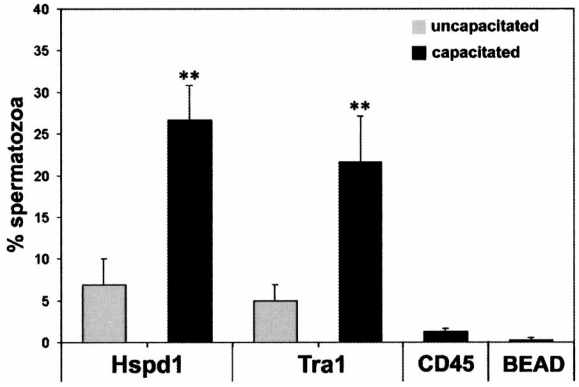

FIG. 7. Capacitation-dependent expression of HSPD1 and TRA1 on the surface of live spermatozoa. Cauda epididymidal sperm were incubated in BWW-HCO_3^- (uncapacitated) or BWW-Ca^{2+}+Sr^{2+} with pentoxifylline and dibutyryl cAMP (capacitated) for 1 h followed by the addition of Protein G beads coated with anti-HSPD1-1 (HSPD1), anti-TRA1-1 (TRA1), anti-CD45 (CD45, negative control), or uncoated (BEAD). Following 30 min of incubation, binding patterns were evaluated by phase contrast microscopy. Beads bound to the head but not to other regions of viable spermatozoa. There was a significant increase in the proportion of sperm labeled with anti-HSPD1-1 and anti-TRA1-1 following capacitation ($P < 0.01$). Controls comprising beads alone or beads coated with a control antibody (CD45) gave significantly lower levels of sperm binding than all other treatments, whether the cells were capacitated ($P < 0.001$) or uncapacitated ($P < 0.05$).

germ cells. Indeed, such a role has been proposed in the testes of rats, humans, and monkeys, all of which display the same HSPD1 localization as described in the current study [14–16]. Additionally, these studies report an apparent loss of HSPD1 from male germ cells during the meiotic stages of spermatogenesis. The mitochondria of male germ cells undergo considerable morphological change during spermiogenesis to prepare for their role in meeting the energy requirements of mature spermatozoa. Mitochondria that do not undergo these changes group together and are excluded from the developing spermatozoa in residual bodies (reviewed in [20]). If the chaperone proteins we have observed in the testis are mitochondrial in origin, they might be lost from differentiating germ cells as a consequence of the mitochondrial remodeling that accompanies spermiogenesis, as well as the ultimate removal of remaining mitochondria in the residual bodies. Labeling of testicular sections with anti-TRA1-1 and anti-TRA1-2 showed staining of spermatogonia, spermatocytes, spermatids, and residual bodies. However, as with anti-HSPD1-1, mature spermatozoa were not labeled with either antibody. TRA1 is an abundant calcium-binding, endoplasmic reticulum glycoprotein believed to function in the translocation of nascent proteins across the endoplasmic reticulum membrane [21, 22] and the folding of denatured proteins as well as in multimer assembly [23]. TRA1 present in developing germ cells during spermatogenesis could be modulating protein biosynthesis and export in the endoplasmic reticulum of

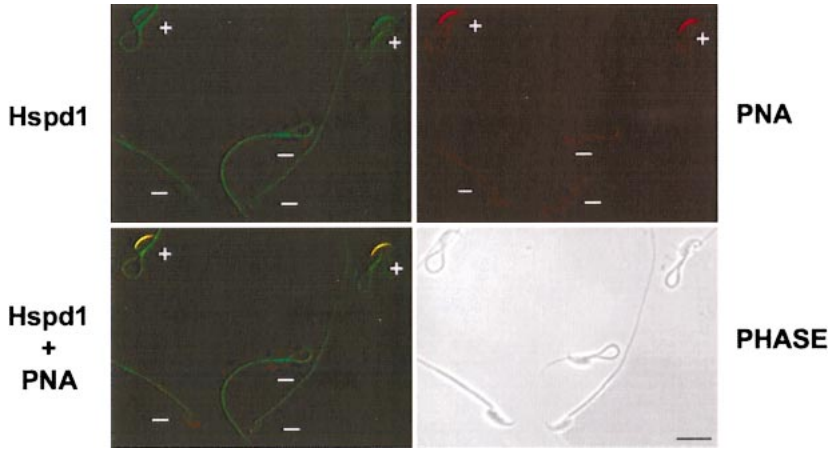

FIG. 8. Correlation between acrosomal status and chaperone labeling of spermatozoa. Cauda epididymidal sperm were incubated in BWW for 1 h followed by 15 min with 1.25 μM A23187. Cells were fixed, stained for anti-HSPD1-1 or anti-TRA1-1, followed by an FITC-conjugated secondary antibody, and counterstained with TRITC-conjugated *Arachis hypogaea* lectin (PNA). Representative images of HSPD1-1/PNA dual labeling are shown. All cells that were positive for HSPD1-1 on the head stained with PNA (+), whereas all cells that did not exhibit HSPD1-1 head labeling were PNA negative (−). The same labeling pattern was observed following staining with TRA1-1 (data not shown). A minimum of 200 cells were scored for each treatment. Bar = 10 μm.

these cells followed by removal in residual bodies. An alternative explanation is that HSPD1 and TRA1 are not detected in testicular sperm due to epitope masking, despite our attempts at several methods of antigen retrieval. Whether these chaperones are physically lost or modified in such a way that the cognate epitopes are not expressed cannot be easily resolved at this stage. In this context, Western blot analysis would have been informative if purified populations of testicular spermatozoa could have been prepared. However, despite many attempts using a variety of protocols, we were singularly unsuccessful in preparing purified populations of testicular spermatozoa.

By contrast, purified sperm populations could be prepared from all three regions of the epididymis. In these populations, the presence of HSPD1 and TRA1 was confirmed by immunocytochemistry as well as by Western blot analysis. No variation in expression levels between epididymal regions was detectable, and no changes in the molecular weight of either protein were apparent. Thus, within the limits of detection of this method, neither HSPD1 nor TRA1 undergo posttranslational modifications in spermatozoa in different regions of the epididymis, which might account for the observed differences in epitope distribution. Similarly, no differences in protein expression were detected between total testicular extracts and cauda epididymidal sperm, suggesting that the same isoforms are present in the testis and epididymis.

As reported earlier [8], HSPD1 and TRA1 are expressed on the head of cauda spermatozoa. The current analysis found that when epididymidal sections were stained with anti-HSPD1-1 and anti-TRA1-1, both chaperones were localized to the head of spermatozoa in the caput, corpus, and cauda epididymides. Taken together with the localization data presented in Figure 1, these results seem to indicate an intriguing phenomenon whereby HSPD1 and TRA1 disappear from germ cells in the testis and reappear in the epididymis. The expression of both these chaperones on spermatozoa in the male reproductive tract appears to be regulated in the same manner, and their distinct expression patterns may indicate discrete spermatogenic and epididymal functions for these proteins. If HSPD1 and TRA1 are in fact lost from germ cells during spermatogenesis, the chaperone observed on epididymal spermatozoa may then represent new protein, transmitted to the spermatozoa in the efferent ducts or rete testis. This possibility is supported by the observation that the epithelium of the rete testis and efferent duct stains positively for both proteins (data not shown).

A similar replacement mechanism has been previously reported for rat sulfated glycoprotein-2 (SGP-2) [24]. Testicular SGP-2 is secreted by the Sertoli cells and binds to specific receptors on developing germ cells. This isoform of the protein then dissociates from spermatozoa during passage through the rete testis and efferent ducts, where it is endocytosed by epithelial cells, only to be replaced by the epididymal form of SGP-2, which is secreted by epithelial principal cells, and binds the same receptors on spermatozoa. Biochemical analysis of testicular and epididymal SGP-2 has revealed that these proteins are of similar molecular weight but exhibit different glycosylation patterns. In the present study, it is possible that testicular and epididymal versions of HSPD1 and TRA1 exist. An alternative explanation for the loss of these proteins in testicular spermatozoa and subsequent reappearance in epididymal spermatozoa could simply involve sequestration of the epitope targeted by anti-HSPD1-1/anti-TRA1-1 during spermiogenesis followed by its reemergence as a result of the plasma membrane remodeling events that occur during epididymal transit (reviewed in [25]).

Immunofluorescence of testicular and epididymal sections using anti-HSPD1-2 yielded notably different results from the HSPD1-1 antibody. This antibody did not label testicular sections or spermatozoa on epididymal sections. Rather, labeling was concentrated in discrete areas within the epididymal lumen. Similarly, immunofluorescence of epididymal sections with anti-TRA1-2 revealed labeling of discrete areas within the epididymal lumen but no labeling of spermatozoa. These areas, which we termed dense bodies, did not appear to be physically associated with the spermatozoa present in the lumen, but rather, they seemed to be suspended in the epididymal fluid. The dense bodies first appeared in the proximal corpus epididymis and persisted throughout the cauda epididymis and vas deferens. These structures were further investigated by electron microscopy, as discussed below.

Transmission electron microscopy and immunogold labeling were used to characterize the dense bodies in the epididymal lumen. These structures averaged approximately 900 nm in diameter and were not membrane-bound, distinguishing them from the smaller, previously described epididymal secretory vesicles termed epididymosomes [26, 27], which we have measured in the mouse to have an average diameter of 100 nm. The dense bodies were visible as individual electron-dense structures suspended in the epididymal lumen, juxtapositioned to, but independent of, the spermatozoa. These structures stained heavily with anti-HSPD1-1 and anti-TRA1-1. Electron microscopic analysis confirmed their restricted localization to the corpus and cauda epididymis, and to the vas deferens, with none apparent in the caput. The presence of a dense, filamentous material in the epididymis has been observed previously in the rat. An early study by Cooper and Hamilton [28] observed that spermatozoa in the vas deferens are ''embedded within a dense material.'' More recently, a similar material present in the rat epididymis was found to contain DE, a glycoprotein secreted by the corpus epididymis involved in sperm maturation and rosette formation in the epididymis [29, 30]. Whether the dense bodies observed here in the mouse epididymis contain a similar glycoprotein content has yet to be determined.

The origin of the dense bodies observed in the current study is unclear. Their lack of plasma membrane suggests that they are not apical blebs, typical of apocrine secretory processes in the epididymis [31, 32]. It is even possible that the dense bodies are not secreted at all, but represent the accretion of proteins present in the epididymal lumen into multimolecular complexes, a process that could be mediated by the chaperone proteins evident within these structures. Accumulation into a single mass could be a way of efficiently and simultaneously delivering a number of proteins to spermatozoa through the mediation of HSPD1, TRA1, and possibly other chaperones present within the dense bodies. While the appearance of dense bodies in the lumen of the proximal corpus coincides with the acquisition of key sperm functions including motility and zona recognition [33–38], as yet, we have no evidence to support their direct involvement in such processes. However, we do know that while the induction of tyrosine phosphorylation in mature spermatozoa is associated with the surface expression of zona recognition sites [8], tyrosine phosphorylation of caput cells does not achieve the same result [39]. Evidently, as spermatozoa pass into the corpus epididymis

they must acquire key proteins that are necessary to link tyrosine phosphorylation with zona receptor expression. Our current hypothesis is that these factors are to be found in the dense bodies, whose appearance in the epididymal lumen coincides with the acquisition of functionality.

If HSPD1 and TRA1 are instrumental in gamete interaction, they should be expressed on the surface of capacitated spermatozoa. An immunobead assay confirmed the results of previous biotinylation experiments in showing that both proteins are present on the sperm surface following capacitation [8]. That this expression pattern is lost once spermatozoa have lost their acrosome further strengthens the concept that these chaperones are expressed on the surface of capacitated spermatozoa. Approximately 25% of the sperm population expressed surface chaperones after almost 2 h in capacitation medium. An inherent feature of mouse sperm populations is their heterogeneity, thus at any single time point, it is expected that cells at various maturational stages will be present. The sperm-expressing surface chaperones are believed to represent that subpopulation capable of interacting with and binding to the zona pellucida.

Molecular chaperones are now being implicated in cell surface signaling in a range of cell types, including cancer cells, blood cells, and fibroblasts [40–45]. Moreover, chaperone proteins GRP94 (TRA1), GRP98, calreticulin, and HSP90 have recently been described on the surface of the mouse oocytes, offering further evidence for chaperone-mediated events in the regulation of mammalian fertilization [46]. Our current studies, aimed at the molecular characterization of proteins associating with HSPD1 and TRA1 that are chaperoned to the sperm surface during capacitation, should further elucidate the molecular basis of sperm-egg recognition.

REFERENCES

1. Dacheux JL, Gatti JL, Dacheux F. Contribution of epididymal secretory proteins for spermatozoa maturation. Microsc Res Tech 2003; 61: 7–17.
2. Austin CR. The ''capacitation'' of the mammalian sperm. Nature 1952; 170:326.
3. Chang M. Fertilizing capacity of spermatozoa deposited into the fallopian tubes. Nature 1951; 168:697–698.
4. McLeskey SB, Dowds C, Carballada R, White RR, Saling PM. Molecules involved in mammalian sperm-egg interaction. Int Rev Cytol 1998; 177:57–113.
5. Wassarman PM. Mammalian fertilization: molecular aspects of gamete adhesion, exocytosis, and fusion. Cell 1999; 96:175–183.
6. Aitken RJ. The complexities of conception. Science 1995; 269:39–40.
7. Thaler CD, Cardullo RA. The initial molecular interaction between mouse sperm and the zona pellucida is a complex binding event. J Biol Chem 1996; 271:23289–23297.
8. Asquith KL, Baleato RM, Nixon B, McLaughlin EA, Aitken RJ. Tyrosine phosphorylation activates surface chaperones facilitating sperm-zona recognition. J Cell Sci 2004; 117:3635–3644.
9. Visconti PE, Bailey JL, Moore GD, Pan D, Olds-Clarke P, Kopf GS. Capacitation of mouse spermatozoa. I. Correlation between the capacitation state and protein tyrosine phosphorylation. Dev Suppl 1995; 121:1129–1137.
10. Aitken RJ, Paterson M, Fisher H, Buckingham DW, van Duin M, Ahmad K. Redox regulation of tyrosine phosphorylation in human spermatozoa and its role in the control of human sperm function. J Cell Sci 1995; 108:2017–2025.
11. Kalab P, Peknicova J, Geussova G, Moos J. Regulation of protein tyrosine phosphorylation in boar sperm through a cAMP-dependent pathway. Mol Reprod Dev 1998; 51:304–314.
12. Mahony MC, Gwathmey T. Protein tyrosine phosphorylation during hyperactivated motility of cynomolgus monkey (*Macaca fascicularis*) spermatozoa. Biol Reprod 1999; 60:1239–1243.
13. Lewis B, Aitken RJ. A redox-regulated tyrosine phosphorylation cascade in rat spermatozoa. J Androl 2001; 22:611–622.
14. Meinhardt A, Parvinen M, Bacher M, Aumuller G, Hakovirta H, Yagi A, Seitz J. Expression of mitochondrial heat shock protein 60 in distinct cell types and defined stages of rat seminiferous epithelium. Biol Reprod 1995; 52:798–807.
15. Meinhardt A, Seitz J, Arslan M, Aumuller G, Weinbauer GF. Hormonal regulation and germ cell-specific expression of heat shock protein 60 (hsp60) in the testis of macaque monkeys (*Macaca mulatta* and *M. fascicularis*). Int J Androl 1998; 21:301–307.
16. Werner A, Seitz J, Meinhardt A, Bergmann M. Distribution pattern of HSP60 immunoreactivity in the testicular tissue of infertile men. Anat Anz 1996; 178:81–82.
17. Biggers JD, Whitten WK, Whittingham DG. The culture of mouse embryos in vitro. In: Daniel JCJ (ed.), Methods in Mammalian Embryology. San Francisco: Freeman Press; 1971:86–116.
18. Laemmli UK. Cleavage of structural proteins during the assembly of the head of bacteriophage T4. Nature 1970; 227:680–685.
19. Towbin H, Staehelin T, Gordon J. Electrophoretic transfer of proteins from polyacrylamide gels to nitrocellulose sheets: procedure and some applications. Proc Natl Acad Sci U S A 1979; 76:4350–4354.
20. Meinhardt A, Wilhelm B, Seitz J. Expression of mitochondrial marker proteins during spermatogenesis. Hum Reprod Update 1999; 5:108–119.
21. Koch G, Smith M, Macer D, Webster P, Mortara R. Endoplasmic reticulum contains a common, abundant calcium-binding glycoprotein, endoplasmin. J Cell Sci 1986; 86:217–232.
22. Mazzarella RA, Green M. ERp99, an abundant, conserved glycoprotein of the endoplasmic reticulum, is homologous to the 90-kDa heat shock protein (hsp90) and the 94-kDa glucose regulated protein (GRP94). J Biol Chem 1987; 262:8875–8883.
23. Nigam SK, Goldberg AL, Ho S, Rhode MF, Bush KT, Sherman MY. A set of endoplasmic reticulum proteins possessing properties of molecular chaperones includes Ca(2+)-binding proteins and members of the thioredoxin superfamily. J Biol Chem 1994; 269:1744–1749.
24. Sylvester SR, Morales C, Oko R, Griswold MD. Localization of sulfated glycoprotein-2 (clusterin) on spermatozoa in the reproductive tract of the male rat. Biol Reprod 1991; 45:195–207.
25. Jones R. Plasma membrane structure and remodelling during sperm maturation in the epididymis. J Reprod Fertil Suppl 1998; 53:73–84.
26. Frenette G, Lessard C, Sullivan R. Selected proteins of ''prostasome-like particles'' from epididymal cauda fluid are transferred to epididymal caput spermatozoa in bull. Biol Reprod 2002; 67:308–313.
27. Saez F, Frenette G, Sullivan R. Epididymosomes and prostasomes: their roles in posttesticular maturation of the sperm cells. J Androl 2003; 24:149–154.
28. Cooper TG, Hamilton DW. Phagocytosis of spermatozoa in the terminal region and gland of the vas deferens of the rat. Am J Anat 1977; 150:247–268.
29. Fornes MW, Burgos MH. Epididymal glycoprotein involved in rat sperm association. Mol Reprod Dev 1994; 38:43–47.
30. Fornes MW, Burgos MH. Sperm association in the rat epididymis. Microsc Electron Biol Celular 1990; 14:115–129.
31. Hermo L, Jacks D. Nature's ingenuity: bypassing the classical secretory route via apocrine secretion. Mol Reprod Dev 2002; 63:394–410.
32. Manin M, Lecher P, Martinez A, Tournadre S, Jean C. Exportation of mouse vas deferens protein, a protein without a signal peptide, from mouse vas deferens epithelium: a model of apocrine secretion. Biol Reprod 1995; 52:50–62.
33. Pavlok A. Development of the penetration activity of mouse epididymal spermatozoa in vivo and in vitro. J Reprod Fertil 1974; 36:203–205.
34. Hoppe PC. Fertilizing ability of mouse sperm from different epididymal regions after washing and centrifugation. J Exp Zool 1975; 192: 219–222.
35. Burkin HR, Miller DJ. Zona pellucida protein binding ability of porcine sperm during epididymal maturation and the acrosome reaction. Dev Biol 2000; 222:99–109.
36. Mahony MC, Oehninger S, Doncel G, Morshedi M, Acosta A, Hodgen GD. Functional and morphological features of spermatozoa microaspirated from the epididymal regions of cynomolgus monkeys (*Macaca fascicularis*). Biol Reprod 1993; 48:613–620.
37. Saling PM. Development of the ability to bind zonae pellucidae during epididymal maturation: reversible immobilization of mouse spermatozoa by lanthanum. Biol Reprod 1982; 26:429–436.
38. Peterson RN, Russell LD, Hunt WD. Evidence for specific binding of

uncapacitated boar spermatozoa to porcine zonae pellucidae in vitro. J Exp Zool 1984; 231:137–147.
39. Ecroyd H, Asquith KL, Jones RC, Aitken RJ. The development of signal transduction pathways during epididymal maturation is calcium dependent. Dev Biol 2004; 268:53–63.
40. Wiest DL, Burgess WH, McKean D, Kearse KP, Singer A. The molecular chaperone calnexin is expressed on the surface of immature thymocytes in association with clonotype-independent CD3 complexes. EMBO J 1995; 14:3425–3433.
41. Shin BK, Wang H, Yim AM, Le Naour F, Brichory F, Jang JH, Zhao R, Puravs E, Tra J, Michael CW, Misek DE, Hanash SM. Global profiling of the cell surface proteome of cancer cells uncovers an abundance of proteins with chaperone function. J Biol Chem 2003; 278:7607–7616.
42. Okazaki Y, Ohno H, Takase K, Ochiai T, Saito T. Cell surface expression of calnexin, a molecular chaperone in the endoplasmic reticulum. J Biol Chem 2000; 275:35751–35758.
43. Ferrarini M, Heltai S, Zocchi MR, Rugarli C. Unusual expression and localization of heat-shock proteins in human tumor cells. Int J Cancer 1992; 51:613–619.
44. Essex DW, Chen K, Swiatkowska M. Localization of protein disulfide isomerase to the external surface of the platelet plasma membrane. Blood 1995; 86:2168–2173.
45. Altmeyer A, Maki RG, Feldweg AM, Heike M, Protopopov VP, Masur SK, Srivastava PK. Tumor-specific cell surface expression of the-KDEL containing, endoplasmic reticular heat shock protein gp96. Int J Cancer 1996; 69:340–349.
46. Calvert ME, Digilio LC, Herr JC, Coonrod SA. Oolemmal proteomics—identification of highly abundant heat shock proteins and molecular chaperones in the mature mouse egg and their localization on the plasma membrane. Reprod Biol Endocrinol 2003; 1:27.